MOLECULAR AND CELLULAR BIOLOGY, Aug. 1995, p. 4375–4384 Vol. 15, No. 8
0270-7306/95/$04.00+0

Accessibility of a Glucocorticoid Response Element in a Nucleosome Depends on Its Rotational Positioning

QIAO LI AND ÖRJAN WRANGE*

Department of Cell and Molecular Biology, Medical Nobel Institute, Karolinska Institute, S-171 77 Stockholm, Sweden

Received 20 March 1995/Returned for modification 26 April 1995/Accepted 19 May 1995

Gene expression requires binding of transcription factors to their cognate DNA response elements, the latter being often integrated into sequence-specifically positioned nucleosomes. To investigate the constraints imposed on factor-DNA recognition by the nucleosomal organization, we studied the binding of glucocorticoid receptor to a single glucocorticoid response element (GRE) displaying four different rotational frames in three different translational positions in reconstituted nucleosomes. We demonstrate that rotational setting of the GRE per se is important for its accessibility. Furthermore, the effects of rotational positioning of the GRE are different for different translational positions of the GRE in the nucleosome. A GRE placed near the nucleosomal dyad is totally blocked by rotating it 180 so that the major groove of the GRE faces the histone octamer. If, on the other hand, the GRE is placed about 40 bp from the nucleosome dyad, then the 180 rotation of the GRE still allows glucocorticoid receptor binding, albeit with a sixfold lower affinity than the peripherally oriented GRE. This suggests that both the rotational positioning and the translational positioning function as a framework for transcription factor response elements in gene regulation.

In the eukaryotic cell nucleus the DNA is organized into nucleosomes which are sequence-specifically positioned in certain regulatory regions (42). A transcription factor response element within such a nucleosome has a defined location relative to the nucleosome dyad (translational positioning) and, as an effect of the helical path of the DNA double helix, a defined orientation relative to the surface of the histone octamer (rotational positioning).

Transcriptional repression mediated by nucleosomes has been demonstrated in several in vivo studies (1, 9, 28, 43). In *Saccharomyces cerevisiae*, the *CUP1* and *HIS3* genes were fully induced by reduction of nucleosome density, achieved by inhibition of the synthesis of histone H4 (9). In the *PHO5* promoter, four strictly positioned nucleosomes are removed or reorganized during gene induction (12). Mutational analysis has demonstrated that the insertion of a more stable nucleosome virtually abolishes *PHO5* inducibility, whereas introduction of an unstable nucleosome results in a leaky promoter with a higher maximal induction capacity (43). Other cellular events are also affected by chromatin structure; for example, DNA replication can be inhibited by a positioned nucleosome (41), and retrovirus integration can be precisely directed even to the base pair level by a positioned nucleosome in vivo (32). The same is true for the human immunodeficiency virus integrase activity in vitro (31).

Induction of transcription often involves rearrangement of chromatin around the promoter and/or upstream segments into a more open structure as revealed by a localized hypersensitivity for DNase I. This is observed within minutes of glucocorticoid hormone induction in the mouse mammary tumor virus promoter (48). The same phenomenon is seen in the glucocorticoid response element (GRE) region of the rat tyrosine aminotransferase gene (5, 33). In both cases the hormone-responsive enhancer is within a positioned nucleosome(s) in the repressed state and the nucleosome(s) becomes structurally altered upon induction (5, 33, 34).

What are the constraints on transcription factor-DNA recognition in a nucleosomal context? Several in vitro studies have addressed the issue in binding experiments using purified protein and in vitro-reconstituted nucleosomes. These studies have shown that different transcription factors possess different inherent capacities to recognize their corresponding DNA segments within a nucleosome. The glucocorticoid receptor (GR) has a two- to fivefold lower affinity to the reconstituted mouse mammary tumor virus nucleosome compared with its affinity to free mouse mammary tumor virus DNA (27, 30). For the transcription factor SP1 the reduction in affinity for a nucleosomal site is 10- to 20-fold (18), while for heat shock factor (HSF) the reduction is at least 100-fold (44). The TATA-box binding protein (TBP) has no detectable affinity for its target site within a nucleosome (15). Furthermore, TFIIIA was shown to bind to its target site in the 5S RNA gene when placed in the peripheral region of a histone H3/H4 tetramer but could not bind to the more centrally located TFIIIA target site in a nucleosome (17). Likewise, GAL4 was shown to bind with lower affinity to a nucleosomal site near the dyad than to a more distal site (6). It seems that positioning of a target site close to the nucleosome dyad leads to stronger inhibition of the factor binding than a more peripheral positioning. However, the affinity of GR for a GRE positioned at the nucleosome dyad is only 1.4-fold lower than its affinity for a GRE located 40 bp from the dyad (19).

In this study we have examined the role of rotational positioning on the recognition of DNA response elements by transcription factors using GR-GRE interaction as a model system. We demonstrate that different rotational settings of the GRE have distinct effects on GR-GRE binding affinity in a nucleosome context. Furthermore, the effects of rotational positioning of the GRE are different for different translational positions of the GRE in the nucleosome. A GRE placed near the nucleosomal dyad is totally blocked by rotating it 180° so that the major groove faces the histones. If, on the other hand, the GRE is placed about 40 bp from the nucleosome dyad, then a

* Corresponding author. Phone: 46 8 728 73 73. Fax: 46 8 31 35 29. Electronic mail address: orjan.wrange@cmb.ki.se.

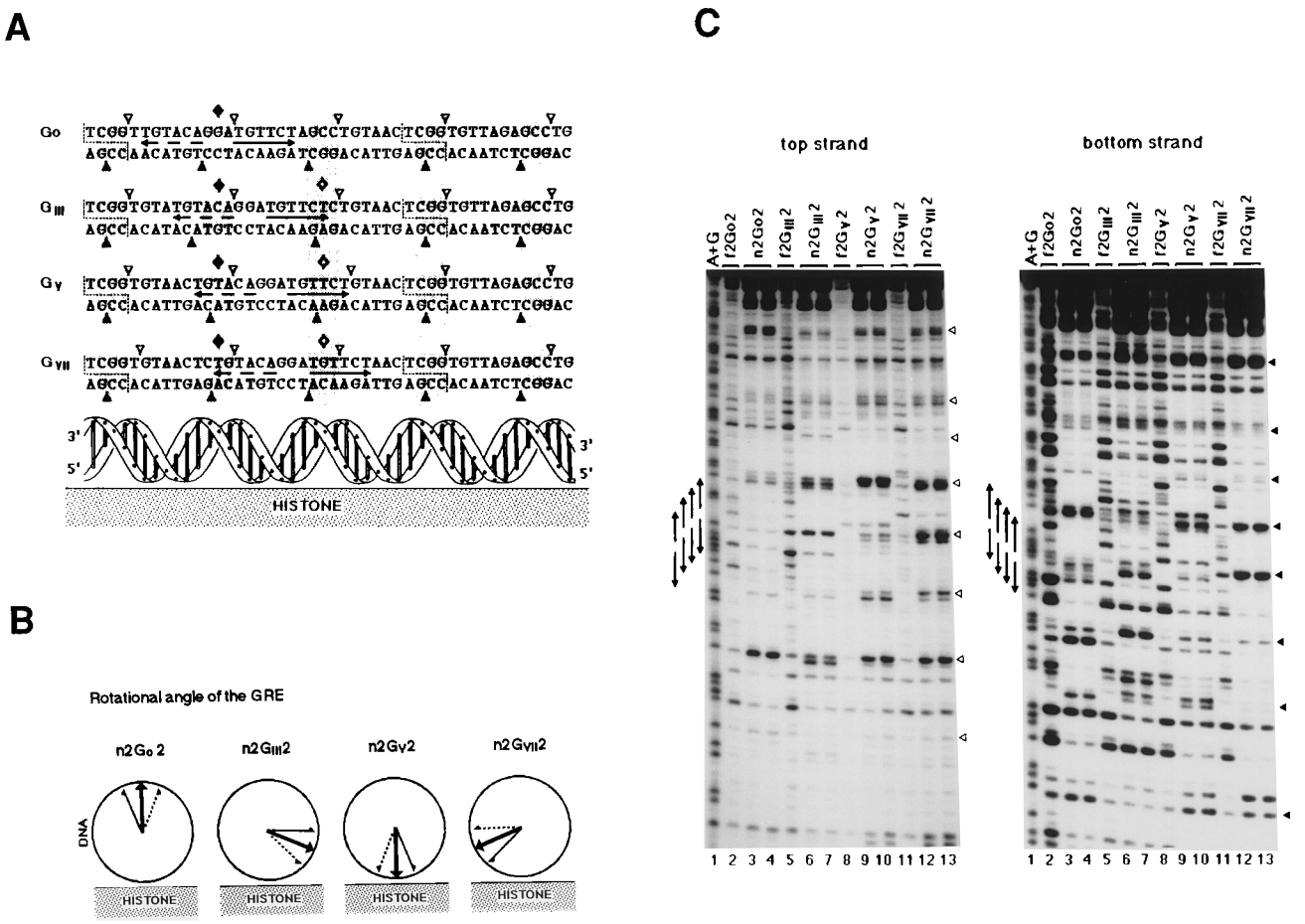

FIG. 1. Rotational positioning of n2Go2, n2G_{III}2, n2G_V2, and n2G_{VII}2. (A) DNase I patterns on n2Go2, n2G_{III}2, n2G_V2, and n2G_{VII}2. The rotational frames of the GRE in different nucleosomes are illustrated according to DNase I cleavage from the top (open arrowheads) and bottom (solid arrowheads) DNA strands. Solid and dashed arrows, perfect and imperfect GR-binding hexanucleotides, respectively. The asymmetric *Ava*I sites used to make the constructs are indicated (dashed zigzags). Diamonds, locations of the nucleosome dyad assessed by exonuclease III protection analysis (Fig. 2). Minor grooves facing the periphery are shaded. (B) Rotational angles of the GRE in the four helical settings. The circles represent the DNA double helix projected in parallel with its length axis. Solid and dashed half-barbed arrows, rotational angles of the perfect (TGTTCT) and the imperfect (TGTACA) hexanucleotides recognized by GR, respectively. Solid arrows, rotational angle of the GRE dyad. (C) DNase I footprinting of the top and bottom DNA strands. Histone-induced DNase I cleavages (arrowheads) are shown for n2Go2 (lanes 3 and 4), n2G_{III}2 (lanes 6 and 7), n2G_V2 (lanes 9 and 10), and n2G_{VII}2 (lanes 12 and 13). Free DNAs f2Go2 (lane 2), f2G_{III}2 (lane 5), f2G_V2 (lane 8), and f2G_{VII}2 (lane 11) were included as a control. Lane A+G, sequencing ladder. Arrows, positions of the partial palindromic GRE in n2Go2, n2G_{III}2, n2G_V2, and n2G_{VII}2 from left to right.

180° rotation of the GRE still allows GR binding, albeit with a sixfold lower affinity than the opposite orientation. We conclude that nucleosome positioning determines GR-GRE binding affinity. This is likely the case for all transcription factors albeit in a factor-specific fashion. Positioned nucleosomes thus may have important functions in gene expression by organizing the topology of regulatory regions.

MATERIALS AND METHODS

Plasmids. To direct rotational positioning of a GRE in the nucleosome, five oligonucleotides were used: TG (TCGGTGTTAGAGCCTGTAAC), Go (TCGGTTGTACAGGATGTTCTAGCCTGTAAC), G_{III} (TCGGTGTATGTACAGGATGTTCTCTGTAAC), G_V (TCGGTGTAACTGTACAGGATGTTCTGTAAC), and G_{VII} (TCGGTGTAACTCTGTACAGGATGTTCTAAC). Plasmids 2Go2, 2G_{III}2, 2G_V2, 2G_{VII}2, 3Go1, 3G_{III}1, 3G_V1, 3G_{VII}1, Go4, G_{III}4, G_V4, and G_{VII}4 were constructed by sequential cloning of TG, Go, G_{III}, G_V, and G_{VII} into the pGEM-Q2 vector (19) at the asymmetric *Ava*I site. The designations include the number of 20-bp TG motifs and their relation to a rotationally positioned GRE.

Nucleosome reconstitution and nuclease digestion. Nucleosome reconstitution, mobility retardation assay (19), DNase I footprinting (4), GR protein purification from rat liver (27), and the determination of the fraction of GR-GRE binding activity in the GR preparation (19) were carried out as described previously. Exonuclease III (Pharmacia Biotechnology) protection analysis was performed with 1.5 fmol of 5′-labelled free or nucleosomal DNA and 15 U of the enzyme per ml in 100 μl of TGDI buffer (20 mM Tris-HCl [pH 7.6], 10% [vol/vol] glycerol, 5 mM dithiothreitol, and 0.1 mg of porcine insulin per ml; kindly donated by NovoNordisk) at 25°C.

DMS methylation protection. 5′-labelled free or nucleosomal DNA was incubated with GR at 25°C for 45 min in 20 μl of GR binding buffer (50 mM NaCl, 1 mM Na_2EDTA, 20 mM Tris-HCl [pH 7.6], 10% [vol/vol] glycerol, 5 mM dithiothreitol, and 0.1 mg of porcine insulin per ml). The binding reaction was then modified by 50 mM dimethyl sulfate (DMS) at room temperature for 3 min, and the modification was stopped by addition of 100 μl of a stop mix (25 mM EDTA, 1.5 M NH_4 acetyl, and 2.8 mM β-mercaptoethanol) and 250 μl of ethanol. The G→A cleavage reaction and the G cleavage reaction were performed as described previously (22). Finally the cleavage patterns were resolved on a 6% sequencing gel.

Quantification. DNase I footprinting and DMS methylation protection were quantified by PhosphorImager analysis with Image Quant version 3.0 and the Fast scan system (Molecular Dynamics) (16).

RESULTS

Rotational GRE setting in reconstituted nucleosomes directed by a DNA-bending sequence. A synthetic DNA-bending sequence having a 10-bp periodicity of $(A/T)_3NN(G/C)_3NN$, referred to as the TG motif, is known to direct rotational

setting of DNA on a histone octamer so that A/T segments are located at sites of minor-groove compression and G/C segments are located at sites of major-groove compression (40). We have previously shown that 95 bp of the TG motif can be used to direct a 15-bp GRE into a defined helical setting in reconstituted nucleosomes (19).

Here we employed the same strategy to position the 15-bp GRE in four different rotational frames within reconstituted nucleosomes. The dyad of the GRE was first placed 10 bp from the G/C triplet(s) of the flanking TG motif (Go; Fig. 1A). Consequently, the two major grooves of the partially palindromic GR recognition sequence, which flank both sides of the 3-bp intervening sequence, are oriented in an outward configuration, away from the histone octamer. Two additional blocks of the TG motif (20 bp each) were then placed on each side of the Go, producing 2Go2. Three other types of rotational variants were generated by moving the GRE dyad 3 bp (G_{III}), 5 bp (G_V), or 7 bp (G_{VII}) away from the Go configuration within the TG motif (Fig. 1A). If the 95 bp of the TG motif determines the rotational setting, the GRE dyad would be forced to rotate from the outward orientation (0° [Go]) to an angle of 108° (G_{III}), 180° (G_V), or 252° (G_{VII}) (Fig. 1B). This implies that the perfect GR-binding hexanucleotide (TGTTCT), whose GR affinity is higher than that of the imperfect hexanucleotide (TGTACA), would have rotational angles of 90, 162, and 234° for G_{III}, G_V, and G_{VII}, respectively (Fig. 1A and B). That the predicted rotational effect has been obtained can be inferred from the results of a DNase I footprinting analysis of the reconstituted nucleosomes (Fig. 1C). Compared with free DNA (Fig. 1C, lanes f2Go2, $f2G_{III}2$, $f2G_V2$, and $f2G_{VII}2$), the reconstituted nucleosomal DNA has an overall 10-bp periodicity of DNase I cutting (lanes n2Go2, $n2G_{III}2$, $n2G_V2$, and $n2G_{VII}2$). This is due to the preferential cutting of nucleosomal DNA by DNase I at sites of minor grooves facing the periphery. The histone-induced DNase I cuts are located at similar positions in all four constructs and flank the $(G/C)_3$ triplets of the TG motif (Fig. 1C), confirming that the TG motif determines the helical setting of the DNA. There are differences in DNase I cutting patterns in the GRE segments. This can be explained by the sequence preference of DNase I cutting and the fact that each of the four constructs has different portions of the GRE exposed at the minor grooves which face the periphery (Fig. 1C, arrows). The 2- to 4-bp staggering of the DNase I cuts of the top and bottom DNA strands is shown in Fig. 1A and is used to locate the positions where the minor grooves face the periphery (26). We conclude that the rotational angle of the GRE is altered as expected by moving the GRE 3, 5, or 7 bp relative to the TG motif.

Translational positioning of the reconstituted nucleosomes n2Go2, $n2G_{III}2$, $n2G_V2$, and $n2G_{VII}2$ was analyzed by an exonuclease III protection assay (Fig. 2). In n2Go2, in which the GRE faces the periphery, the existence of a single translational position of the histone octamer is indicated by the first histone-induced exonuclease III stop on either strand defining a 144-bp segment of DNA, as reported previously (19). The exonuclease III protection analysis of $n2G_{III}2$, $n2G_V2$, and $n2G_{VII}2$ revealed a more complex pattern, showing histone-induced protection of more than 144 bp of DNA (Fig. 2). Comparison of the protection pattern of the top and bottom DNA strands demonstrates that $n2G_{III}2$, $n2G_V2$, and $n2G_{VII}2$ allow two alternative translational positions, located 10 bp apart (Fig. 2, middle panel), placing the GRE dyad on either side of the nucleosome dyad (Fig. 1A, diamonds). This translational variability is not due to a movement of the GRE dyad away from the nucleosome dyad but, rather, the rotation of the GRE away from a facing-out configuration. This follows from the fact that

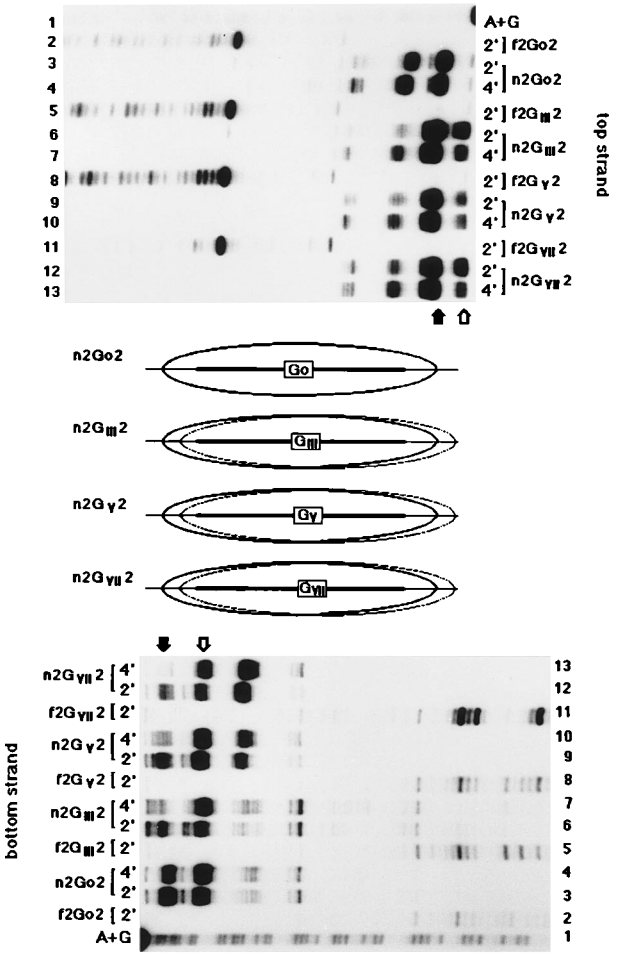

FIG. 2. Translational positions of n2Go2, $n2G_{III}2$, $n2G_V2$, and $n2G_{VII}2$. Exonuclease III protection analysis was performed on the DNA top (upper gel) and bottom (lower gel) strands of n2Go2 (lanes 3 and 4), $n2G_{III}2$ (lanes 6 and 7), $n2G_V2$ (lanes 9 and 10), and $n2G_{VII}2$ (lanes 12 and 13). Free DNAs f2Go2 (lane 2), $fG_{III}2$ (lane 5), $f2G_V2$ (lane 8), and $f2G_{VII}2$ (lane 11) were included as a control. Lane A+G, sequencing ladder. The duration of exonuclease III digestion is indicated in minutes. Solid arrows, histone-induced protection on both the top and the bottom strands as in n2Go2; open arrows, alternatively positioned protection for $n2G_{III}2$, $n2G_V2$, and $n2G_{VII}2$ on both DNA strands. Middle panel, translational positions of histone octamers (ellipsoids) in the indicated nucleosomes. Horizontal lines, 165-bp DNA fragment with the 95 bp of the TG motif (thicker portion) flanking the 15-bp GRE (rectangle).

the same translational variability occurs when a GRE is rotated at a nucleosome domain about 20 or 40 bp from the nucleosome dyad (see below).

The exonuclease III protection analysis showed that, despite the heterogeneity in translational positioning, the rotational positions of the GRE in $n2G_{III}2$, $n2G_V2$, and $n2G_{VII}2$ were homogeneous. This is shown by the fact that the intervals of the various histone-induced exonuclease III stops were 10 bp apart and that the histone-dependent DNase I cleavage pattern was the same within the TG motif.

In conclusion, we have generated four nucleosomal probes: n2Go2, in which the two partially palindromic GR-binding hexanucleotides are in a major-groove facing-out configuration and the GRE dyad coincides with the nucleosome dyad; $n2G_{III}2$, in which the GRE is rotated 108° and translationally positioned either −7 bp or +3 bp relative to the nucleosome dyad; $n2G_V2$, in which the GRE is rotated 180° and transla-

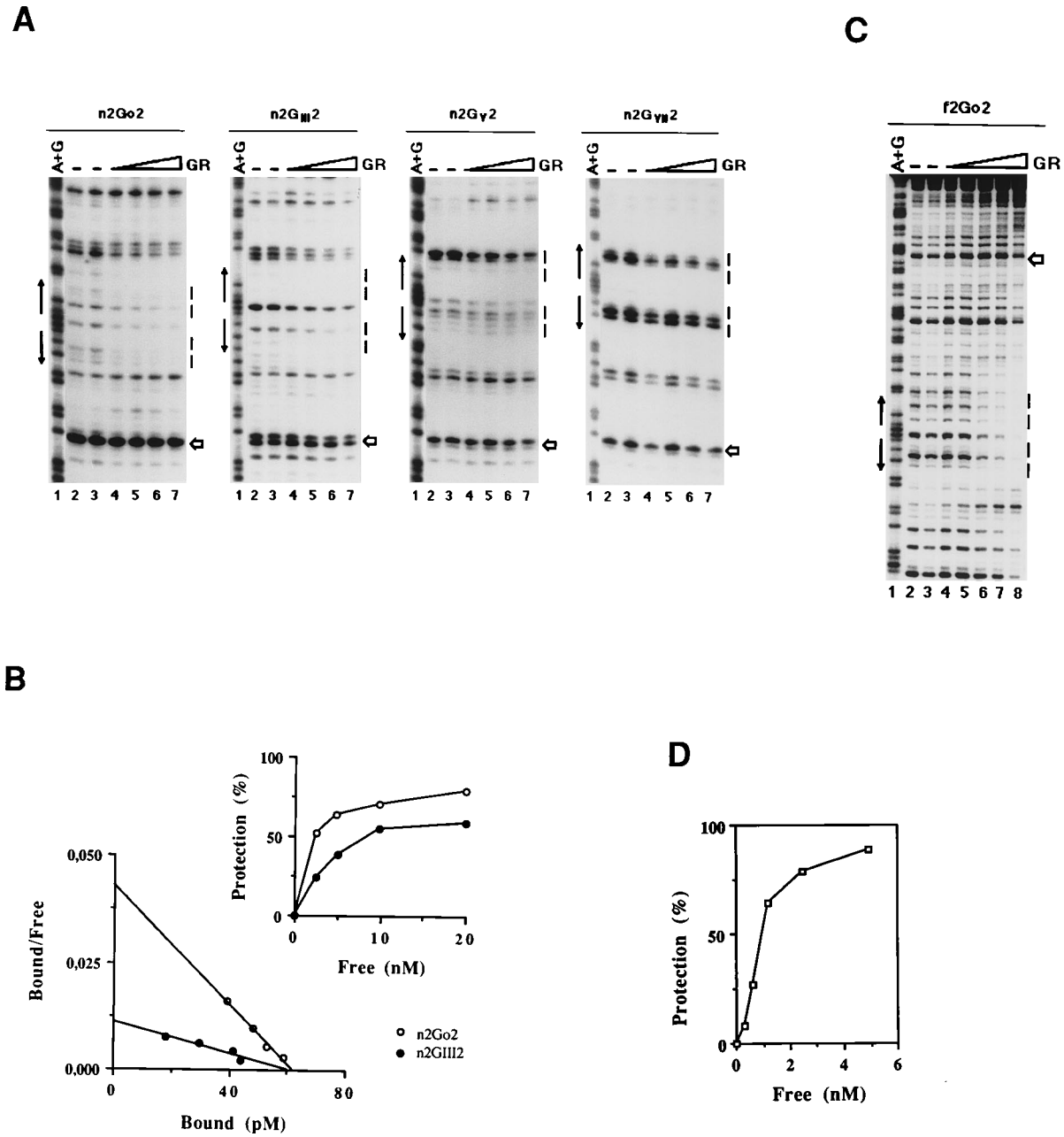

FIG. 3. GR-GRE binding affinity analyzed by quantitative DNase I footprinting. (A) Binding of GR to the indicated nucleosome probes. A constant amount of nucleosome (37.5 pM) was incubated in the absence (lanes 2 and 3) or the presence (2.5, 5, 10, and 20 nM in lanes 4 to 7, respectively) of GR. Vertical arrows, positions of the partially palindromic GRE; dashes, GR-protected region used for affinity analysis; open arrows, reference bands. (B) Quantification of the results in panel A. GR-induced protection is plotted as a function of the free-GR concentration (upper right) or Scatchard analysis (lower left). For n2Go2 and n2G$_{III}$2, the apparent K_ds were 1.4 and 5.8 nM, respectively; the maximal binding was 62 nM for both, and the correlation coefficients were 0.99 and 0.98, respectively. (C) GR binding to free GRE. A constant concentration of f2Go2 (37.5 pM) was incubated in the absence (lanes 2 and 3) or the presence (0.3 to 5 nM in lanes 4 to 8) of GR. The symbols are defined above. (D) Quantification of the results in panel C. GR-induced protection is plotted as function of the free-GR concentration. The apparent K_d for f2Go2 was 0.8 nM (free-GR concentration at half-maximal GRE binding).

tionally positioned either −5 bp or +5 bp relative to the nucleosome dyad; n2G$_{VII}$2, in which the GRE is rotated 252° and translationally positioned either −3 bp or +7 bp relative to the nucleosome dyad (diamonds in Fig. 1A).

Rotational positioning of a nucleosomal GRE determines GR affinity. Quantitative DNase I footprinting was used to evaluate the GR-GRE binding affinity for the reconstituted nucleosomes n2Go2, n2G$_{III}$2, n2G$_{V}$2, and n2G$_{VII}$2. In these experiments increasing amounts of GR (2.5 to 40 nM) were incubated with a constant concentration (37.5 pM) of the indicated nucleosome (Fig. 3A). The results were quantified by PhosphorImager analysis. A distinct GR-induced DNase I protection over the GRE region was observed for n2Go2 and n2G$_{III}$2, whereas no GR-dependent DNase I protection was detected in n2G$_{V}$2 and n2G$_{VII}$2 (Fig. 3A). The extent of protection from DNase I digestion in the GRE region for n2Go2

TABLE 1. GR-GRE binding affinity[a]

DNA	K_d (nM)	B_{max} (pM)	n
f2Go2	0.8 ± 0.1		3
n2Go2	1.5 ± 0.3	66.6 ± 4.0	3
$n2G_{III}2$	7.8 ± 4.6	69.9 ± 6.2	3
$n2G_V2$	>40		3
$n2G_{VII}2$	>40		3
fGo4	0.8 ± 0.2		6
nGo4	1.0 ± 0.6	72.1 ± 6.8	6
$nG_{III}4$	3.6 ± 0.9	50.7 ± 10.7	4
nG_V4	6.2 ± 1.2	60.9 ± 7.1	6
$nG_{VII}4$	>40		4

[a] For free GRE, K_d corresponds to the free GR concentration at half-maximal GRE binding, while for nucleosomal GRE the apparent K_d and maximal binding (B_{max}) were calculated by Scatchard analysis (37).

and $n2G_{III}2$ was plotted as a function of the concentration of free GR and displayed the characteristics of a specific binding reaction (Fig. 3B). GR-induced protection was also determined by Scatchard analysis (37) (Fig. 3B). The apparent dissociation constants (K_d) obtained from this analysis were 1.5 ± 0.3 nM (n = 3) and 7.8 ± 4.6 nM (n = 3) for GR binding to n2Go2 and $n2G_{III}2$, respectively (Table 1). The maximal binding was the same for both n2Go2 and $n2G_{III}2$ (Table 1). The discrepancy in GR affinity for $n2G_{III}2$ and $n2G_{VII}2$ could be explained by the difference in rotational setting of the perfect GR-binding hexanucleotide (TGTTCT), which has higher GR affinity (Fig. 1B).

In contrast to the nucleosomal GRE, the free GREs of f2Go2, $f2G_{III}2$, $f2G_V2$, and $f2G_{VII}2$ displayed no difference in GR-GRE binding affinity as assessed by competition for GR binding with increasing amounts of calf thymus DNA in a mobility retardation assay (Table 2). The apparent dissociation constant of GR for a free GRE was 0.8 ± 0.1 nM (n = 3) on the basis of the free-GR concentration required for half-maximal binding of the GRE inferred from quantitative DNase I footprinting analysis (Table 1; Fig. 3C and D).

We conclude that the rotational setting of a nucleosomal GRE is an important determinant of GR affinity. The highest GR-GRE binding affinity is achieved when the two consecutive major grooves constituting the GRE are facing the periphery. A 108° clockwise rotation of the GRE reduces GR affinity about fivefold (Table 1). Further rotation of the GRE to 180 or 252° abolishes GR binding. The difference in GR binding affinity due to the rotational setting is observed only in a nucleosomal context.

Contacts of GR with nucleosomal GRE. GR binds to the major groove of GRE (21, 38), and the binding of GR prevents DMS methylation of four symmetrically positioned guanines in the TAT GRE (3). Inversely, methylation of these guanines was shown to interfere with GR binding (19). Here we have employed DMS methylation as an additional method to assess specific GR-GRE interaction in a nucleosomal context. GR-induced protection against methylation of a single GRE in free DNA was established for all four constructs, f2Go2, $f2G_{III}2$, $f2G_V2$, and $f2G_{VII}2$ (Fig. 4A). The GR binding reaction mixture contained 2.5 nM GR and 37.5 pM free DNA. GR protected the free GRE at four symmetrically distributed guanines as described above, and the same degree of protection was obtained for all four constructs (Fig. 4A and B). However, there was a distinct difference in the pattern of DMS protection for nucleosomal DNA (Fig. 4C). n2Go2, in which the GRE faces the periphery, displayed a level of DMS protection at the guanine N-7 position that was similar to but lower than the level for free GRE, whereas $n2G_{III}2$ showed asymmetric DMS protection only at guanines of the GRE top strand (Fig. 4D). This alteration in methylation protection might reflect restricted access of GR to a GRE which has been rotated 108°. The difference in GR-GRE contacts thus agrees with the lower GR affinity of $n2G_{III}2$ relative to that of n2Go2 in the DNase I footprinting experiments (Fig. 3B). Also in agreement with these experiments, $n2G_V2$ and $n2G_{VII}2$ showed no GR-induced DMS methylation protection (Fig. 4C). There was no GR-dependent methylation protection at the N-3 positions of adenines, i.e., in the minor groove of the GRE (Fig. 4C).

Effects of rotational GRE positioning about 20 and 40 bp from the nucleosome dyad. The n3Go1 construct contains a single translational position of a GRE, 20 bp from the nucleosome dyad and facing the periphery (19). In this case even the affinity of the peripherally oriented GRE is threefold lower than the affinity of the likewise-oriented GRE at the nucleosome dyad (19). GR binding could not be detected for three other variants ($n3G_{III}1$, $n3G_V1$, and $n3G_{VII}1$) of a rotationally positioned GRE at this translational position (data not shown). The exonuclease III protection analysis revealed the same distribution of two alternative translational positions for these three rotational variants as the distribution for the rotational variants with the GRE located near the dyad (compare Fig. 2 and 5). The GRE dyad is thus placed 13 or 23, 15 or 25, and 17 or 27 bp from the nucleosome dyad in $n3G_{III}1$, $n3G_V1$, and $n3G_{VII}1$, respectively.

GR-GRE binding affinity was also measured as a function of rotational setting when the GRE was positioned about 40 bp from the nucleosome dyad by use of the nGo4, $nG_{III}4$, nG_V4, and $nG_{VII}4$ constructs. In this case the single translational positioning of nGo4 (19) was again altered into two main translational positions for $nG_{III}4$ and nG_V4. Consequently, the GRE dyad was located 37 or 47 bp and 35 or 45 bp from the nucleosome dyad in $nG_{III}4$ and nG_V4, respectively, whereas in $nG_{VII}4$ the GRE had a single translational position with its dyad placed 33 bp from the nucleosome dyad (data not shown). The GR binding affinity for these rotational variants was evaluated by quantitative DNase I footprinting (Fig. 6A). The GR concentrations in these experiments were 1.3 to 20 nM for nGo4 and $nG_{III}4$ and 2.5 to 40 nM for nG_V4 and $nG_{VII}4$. The apparent dissociation constants calculated by Scatchard analysis were 1.0 ± 0.6 nM (n = 6), 3.6 ± 0.9 nM (n = 4), and 6.2 ± 1.2 nM (n = 6) for nGo4, $nG_{III}4$, and nG_V4, respectively, while $nG_{VII}4$ had no detectable affinity for GR (Fig. 6A and Table 1). That GR was indeed making sequence-specific contacts with the GRE in nGo4, $nG_{III}4$, and even nG_V4, in which the GRE faces the histone octamer, was confirmed by the observed GR-dependent DMS methylation protection (Fig.

TABLE 2. Calf thymus DNA competition for GR binding to free GRE[a]

DNA[b]	GR-fGRE (%) at the following concn of CT DNA[c]:	
	3.2 μg/ml	12.8 μg/ml
f2Go2	41.8 ± 3.9	15.7 ± 1.8
$f2G_{III}2$	45.6 ± 9.6	16.8 ± 4.3
$f2G_V2$	45.5 ± 3.1	14.7 ± 3.3
$f2G_{VII}2$	41.8 ± 6.8	14.6 ± 3.6

[a] The mobility retardation assay was performed at a GR concentration of 0.9 nM.
[b] 75 pM. n = 4.
[c] One hundred percent binding was set at 0.8 μg of calf thymus (CT) DNA per ml to eliminate nonspecific GR binding (19). fGRE, free GRE.

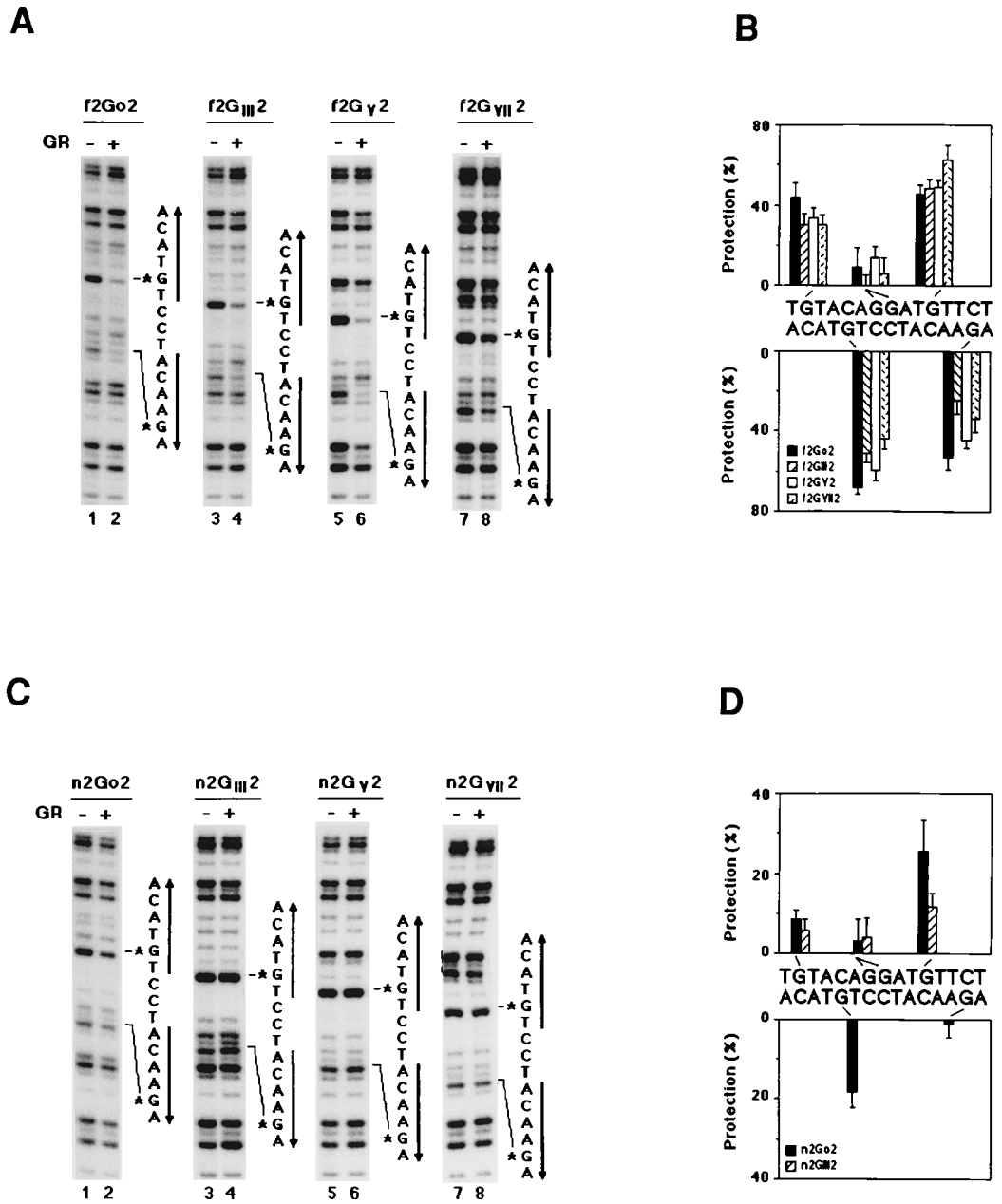

FIG. 4. GR-GRE contacts assessed by DMS methylation protection. (A) GR-dependent methylation protection for the indicated bottom strand of free GRE. The G→A cleavage was performed at a constant concentration of probe (37.5 pM) in the absence (lanes 1, 3, 5, and 7) or the presence (2.5 nM; lanes 2, 4, 6, and 8) of GR. The two protected guanine residues are indicated (*). (B) Quantification of DMS methylation protection of the indicated free GRE for both the top strand (upper panel; $n = 4$) and the bottom strand (lower panel; $n = 5$). (C) GR-dependent methylation protection for the indicated bottom strand of nucleosomal GRE. The experimental design was the same as that for panel A, except that the GR concentration was 10 nM. (D) Quantification of DMS methylation protection of the indicated nucleosomal GREs for both the top strand (upper panel; $n = 5$) and the bottom strand (lower panel; $n = 7$).

6B). Although the GR-induced methylation protection was most pronounced in nGo4, in which the major groove of the GRE faces the periphery, it was also distinct in $nG_{III}4$ and nG_V4, in which the GRE is rotated towards the histone octamer. The methylation protection was totally absent for $nG_{VII}4$, corroborating the DNase I footprinting experiments.

The binding of GR to nG_V4 resulted in not only GR-induced DNase I protection at the GRE region but also GR-dependent DNase I hypersensitivity at a site 21 bp from the GRE dyad (Fig. 6A, arrowhead). This site is not cleaved by DNase I in nucleosomal DNA in the absence of GR but is preferentially cleaved by DNase I in free DNA. This implies that the DNA-histone contacts at this position are disrupted by GR binding.

DISCUSSION

GR binding affinity is determined by the rotational GRE setting when the GRE is positioned near the nucleosome dyad. When the GRE is located at the nucleosome dyad and with its GR-binding sequence positioned in two consecutive major grooves facing the periphery, as in n2Go2, its GR affinity is only twofold lower than that of the same GRE in free DNA

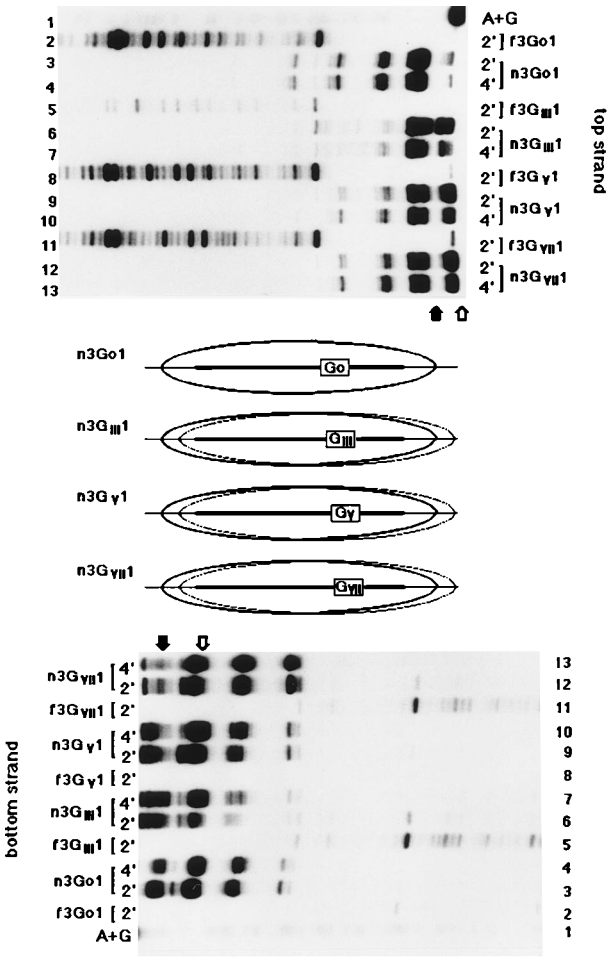

FIG. 5. Translational positions of n3Go1, n3G_{III}1, n3G_V1, and n3G_{VII}1. Exonuclease III protection analysis was performed on the top (upper gel) and bottom (lower gel) DNA strands of the indicated nucleosomes. Free DNAs f3Go1, f3G_{III}1, f3G_V1, and f3G_{VII}1 were included as a control. Lane A+G, sequencing ladder. Exonuclease III digestion times are indicated in minutes. Solid arrows, histone-induced protection on both the top and the bottom DNA strands as in n3Go1; open arrows, alternatively positioned protection for n3G_{III}1, n3G_V1, and n3G_{VII}1 on both DNA strands. Middle panel, translational positions of histone octamers (ellipsoids) on the indicated nucleosomes. Horizontal lines, 165-bp DNA fragment with the 95 bp of the TG motif (thicker portion) flanking the 15-bp GRE (rectangle).

(Table 1). On the other hand, a GRE facing the histone octamer and translationally positioned +5 or −5 bp from peripherally oriented GRE is not accessible for GR binding and can be regarded as functionally closed (Fig. 7). This profound effect of a 180° rotation of the GRE on GR-GRE binding affinity is a logical result when one considers that the two GR subunits in the GR homodimer bind their cognate DNA from the same side. This has been established by X-ray diffraction study of the cocrystal of the DNA binding domain (DBD) of GR with GRE (21).

The rotational angle of the GRE dyad in n2G_{III}2 and n2G_{VII}2 should be the same, i.e., +108 and −108°, respectively, relative to the facing-out mode Go (Fig. 1A and B), and yet there is significant GR binding to the former and no detectable binding to the latter (Table 1 and Fig. 7). The difference is probably caused by the asymmetry of the partially palindromic GRE. It contains one perfect GR-binding hexanucleotide (TGTTCT) and one imperfect hexanucleotide (TGTACA) spaced by 3 bp (Fig. 1A). This places the centers of the two hexanucleotides 9 bp apart and implies a 36° angle between these two GR-binding segments (Fig. 1B) on the basis of a 10-bp helical twist of the TG motif in the nucleosomes (40). It thus makes the perfect GR-binding hexanucleotide, which has higher affinity for GR (45), more accessible for GR binding in n2G_{III}2 than in n2G_{VII}2 (Fig. 1B), a situation which may explain the observed difference in GR-GRE binding affinity.

The effect of rotational GRE setting on GR binding affinity is influenced by the translational positioning. A GRE near the nucleosome dyad, but with its GR binding sequence facing the histones, as in 2G_V2, is functionally closed. However, a GRE with the same rotational setting, but positioned 35 or 45 bp from the nucleosome dyad, is open for GR binding, albeit with an affinity that is sixfold lower affinity than the affinity of the corresponding peripherally oriented GRE (Table 1 and Fig. 7). This shows that rotational setting per se is important but does not alone determine whether binding occurs. Rather, the combination of rotational and translational nucleosome positioning determines the GR-GRE binding affinity. This might be due to heterogeneity along the octamer surface (2), the presence of kinks in the nucleosomal DNA (35), or a sequence-dependent difference in histone-DNA contacts (19). The importance of translational positioning has been reported previously for the n3Go1 construct, which places the GRE dyad 20 bp from the nucleosome dyad and whose affinity for GR is threefold lower than that of n2Go2, in which the GRE dyad is at the nucleosome dyad (19).

GR binding to a GRE rotationally positioned towards the histone octamer. The specific GR-GRE binding in the nG_V4 nucleosome, in which the two major grooves of the GRE face the histone octamer, is an intriguing result. How is it possible for GR, which has a molecular mass of 87.5 kDa (24) and forms a homodimer at the GRE (45, 46), to bind to a target which is facing the histone octamer? Firstly, the GRE dyad in nG_V4 was positioned 35 or 45 bp from the nucleosome dyad, i.e., 37 or 47 bp from the end of the nucleosomal DNA, and at the flank of the TG motif. This implies a weaker interaction between the GRE and the histones than if the GRE is positioned at the nucleosome dyad, as in n2G_V2 (19). Secondly, an electron microscope image of the GR protein showed that the monomer has an elongated structure of 125 to 160 Å (12.5 to 16.0 nm) in length with a thicker portion at each end of about 55 to 70 Å (5.5 to 7.0 nm) in diameter and a very thin central portion, i.e., an hourglass shape (11). The GR DBD, which consists of 66 amino acid residues with a molecular mass of about 7 kDa, has been functionally defined by in vitro mutagenesis and is localized at the central portion of the GR polypeptide (13, 36). The crystal structure of the homodimeric GR DBD–GRE complex (21) suggests that a space of about 18 Å (1.8 nm) is required between the DNA and the histone octamer to accommodate such a DBD when a nucleosomal GRE is facing the histone octamer. On the basis of the astonishingly small distortion of histone-DNA contacts by GR binding, as inferred from DNase I footprinting analysis of nG_V4 (Fig. 6A, arrowhead), we propose that the hourglass-shaped GR monomer is flexible and allows sharp bending to occur on both sides of the thin central DBD. The DBD would then protrude from the bulky ends of the protein and gain access to a spatially restricted GRE, as in nG_V4, via the tunnel formed between the DNA major groove and the histone octamer.

Nucleosome positioning and transcription regulation. Our data show that sequence-specific positioning of a nucleosome allows the accessibility of a GRE to be almost infinitely varied from an open state, with the GR-GRE binding affinity in the range of that seen with free DNA, to a closed state, in which no

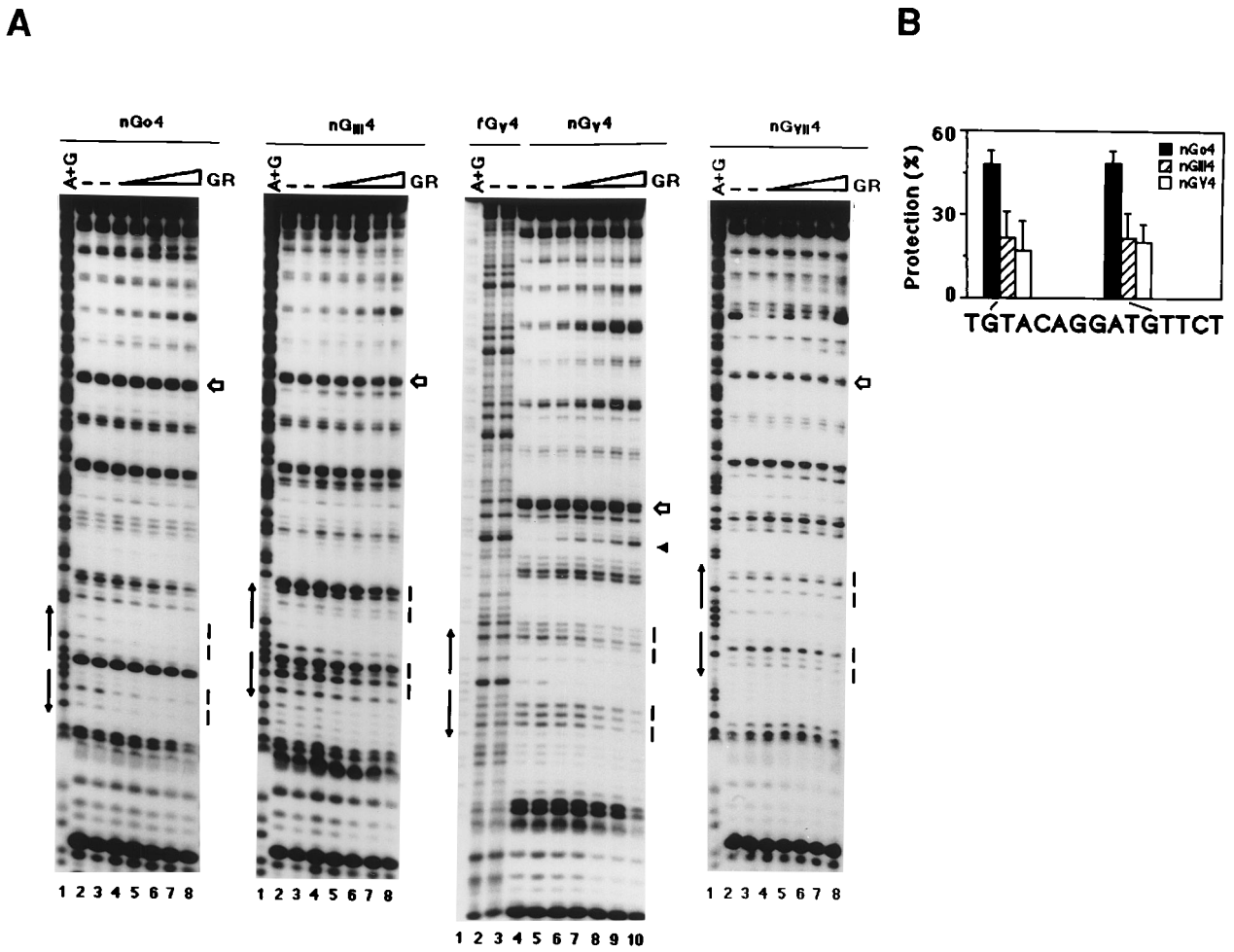

FIG. 6. GR binding to the GRE positioned about 40 bp from the nucleosome dyad. (A) DNase I footprinting analysis of the indicated nucleosomes. A constant amount of nucleosome (37.5 pM) was incubated in the absence (lanes 2 and 3 for nGo4, $nG_{III}4$, and $nG_{VII}4$; lanes 4 and 5 for nG_V4) or the presence (1.3 to 20 nM for nGo4 and $nG_{III}4$ in lanes 4 to 8 or 2.5 to 40 nM for nG_V4 in lanes 6 to 10 and $nG_{VII}4$ in lanes 4 to 8) of GR. Vertical arrows, positions of the partially palindromic GRE; dashes, GR-protected region used for affinity analysis; open arrows, reference bands; solid arrowhead, GR-induced DNase I hypersensitivity site in nG_V4. (B) Quantification of DMS methylation protection for the DNA top strand of nGo4, $nG_{III}4$, and nG_V4 (n = 4). The experiments were carried out at a constant concentration of probes (75 pM) in the absence or the presence (20 nM) of GR.

GR binding can occur. This suggests that a sequence-specifically positioned nucleosome, or an array of nucleosomes, may not only function as a general repressor but also, in other cases, be regarded as a specific presenter which directs the topological arrangement of different DNA response elements in relation to each other. This might be exploited in the tissue-specific enhancer of the serum albumin gene, in which an array of three nucleosomes are sequence-specifically positioned but only in liver tissue, in which this gene is expressed (23). A role of a positioned nucleosome as a structural promoter/enhancer element has also been suggested for the *Drosophila hsp26* promoter (10, 20) and the *Xenopus* vitellogenin B1 promoter (39).

GR has a unique capacity to recognize a GRE in a nucleosome context compared with other transcription factors, e.g., SP1, GAL4-VP16, HSF, NF-1, and TBP (see the introduction). The ability of GR to bind to its target on a histone octamer surface at the nucleosome dyad or to bind even to a GRE rotationally positioned towards the histone octamer 35 or 45 bp from the dyad may be an important aspect of its function as a hormone-inducible transcription factor. In the mouse mammary tumor virus promoter glucocorticoid hormone triggers

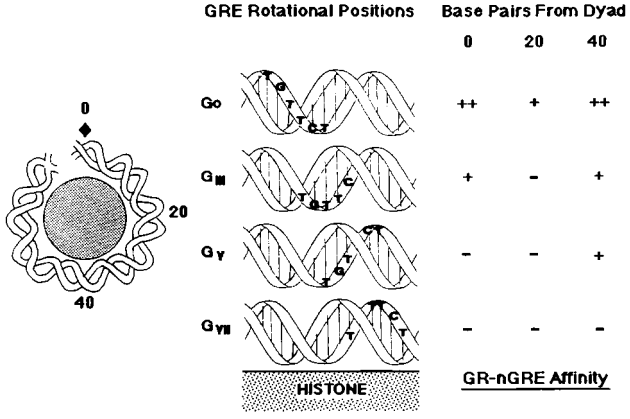

FIG. 7. Nucleosome positioning effects on GR-GRE interaction. Circle, histone octamer; double helix, half of the DNA path in a nucleosome (35), with the base pairs numbered relative to the dyad axis (diamond). The four helical settings of the perfect GR-binding hexanucleotide are shown with the corresponding GR affinities in relation to their translational positions. ++, K_d of 1 to 2 nM; +, K_d of 3 to 8 nM; −, undetectable GR binding at a GR concentration of ≤40 nM.

the disruption of a nucleosome (34) which is necessary to allow NF1 binding (7), even though NF1 binds strongly to free DNA and is constitutively present in the nucleus. This hierarchy, with binding of an inducible transcription factor leading to the binding of other constitutive factors that are otherwise locked out of their binding sites by the chromatin, may be an important strategy to achieve inducible gene regulation.

If chromatin is able to insulate genes from the transcriptional machinery, there must be a system which can mediate site-specific chromatin rearrangement to enable selective gene induction. Binding of GR to its target in a nucleosome does not lead to nucleosome disruption in vitro (27). Recent work has revealed that a cellular multiprotein complex, here referred to as the SWI/SNF complex, may mediate chromatin rearrangement during gene activation (14, 29). A purified SWI/SNF multiprotein complex is able to alter a nucleosome and thereby facilitates binding of GAL4-VP16 (8) or TBP (15) to their cognate DNA binding sites. However, the SWI/SNF complex does not seem to have any sequence-specific DNA binding capacity (8, 15). In the living cell, chromatin rearrangement, perhaps mediated by the SWI/SNF complex, has to be targeted to the correct DNA segment. We suggest GR as a candidate for such a targeting function. Other results which support this hypothesis are findings that GR requires functional SWI/SNF activity for gene induction in a heterologous yeast system and that a GR derivative coprecipitates with SWI3, a component of the SWI/SNF complex (47). Furthermore, GR-mediated transcriptional induction in certain cell lines is enhanced by coexpression of a human homolog to SWI2/SNF2, a component of the SWI/SNF multiprotein complex (25).

In conclusion, we have demonstrated for the first time that the rotational positioning of a single nucleosomal GRE can influence the binding of its cognate factor, GR, from an open state to a closed state. This suggests that positioning of nucleosomes may increase the regulatory repertoire of a given number of transcription factors by orchestrating the factor-binding hierarchy in regulation of gene expression.

ACKNOWLEDGMENTS

We thank Ulla Björk for skillful technical assistance. We are indebted to C. Legraverend and L. Wieslander for critical reading of the manuscript.

This work was supported by a grant from the Swedish Cancer Foundation (2222-B94-10XCC) and by Ingabritt and Arne Lundberg's Foundation.

REFERENCES

1. **Almouzni, G., and A. P. Wolffe.** 1993. Replication-coupled chromatin assembly is required for repression of basal transcription in vivo. Genes Dev. **7:**2033–2047.
2. **Arents, G., and E. N. Moudrianakis.** 1993. Topography of the histone octamer surface: repeating structural motifs utilized in the docking of nucleosomal DNA. Proc. Natl. Acad. Sci. USA **90:**10489–10493.
3. **Becker, P. B., B. Gloss, W. Schmid, U. Strähle, and G. Schütz.** 1986. In vivo protein-DNA interactions in a glucocorticoid response element require the presence of the hormone. Nature (London) **324:**686–688.
4. **Brenowitz, M., D. F. Senear, M. A. Shea, and G. K. Ackers.** 1986. Quantitative DNase footprint titration: a method for studying protein-DNA interactions. Methods Enzymol. **130:**132–181.
5. **Carr, K. D., and H. Richard-Foy.** 1990. Glucocorticoids locally disrupt an array of positioned nucleosomes on the rat tyrosine aminotransferase promoter in hepatoma cells. Proc. Natl. Acad. Sci. USA **87:**9300–9304.
6. **Chen, H., B. Li, and J. L. Workman.** 1994. A histone binding protein, nucleoplasmin, stimulates transcription factor binding to nucleosomes and factor-induced nucleosome disassembly. EMBO J. **13:**380–390.
7. **Cordingley, M. G., A. T. Riegel, and G. L. Hager.** 1987. Steroid-dependent interaction of transcription factors with the inducible promoter of mouse mammary tumor virus in vivo. Cell **48:**261–270.
8. **Côté, J., J. Quinn, J. L. Workman, and C. L. Peterson.** 1994. Stimulation of GAL4 derivative binding to nucleosomal DNA by the yeast SWI/SNF complex. Science **265:**53–60.
9. **Durrin, L. K., R. K. Mann, and M. Grunstein.** 1992. Nucleosome loss activates *CUP1* and *HIS3* promoters to fully induced levels in the yeast *Saccharomyces cerevisiae*. Mol. Cell. Biol. **12:**1621–1629.
10. **Elgin, S. C. R.** 1988. The formation and function of DNase I hypersensitive sites in the process of gene activation. J. Biol. Chem. **263:**19259–19262.
11. **Eriksson, P., B. Daneholt, and Ö. Wrange.** 1991. The glucocorticoid receptor in homodimeric and monomeric form visualised by electron microscopy. J. Struct. Biol. **107:**48–55.
12. **Fascher, K.-D., J. Schmitz, and W. Hörtz.** 1993. Structural and functional requirements for the chromatin transition at the PHO5 promoter in Saccharomyces cerevisiae upon PHO5 activation. J. Mol. Biol. **231:**658–667.
13. **Giguere, V., S. M. Hollenberg, M. G. Rosenfeld, and R. M. Evans.** 1986. Functional domains of the human glucocorticoid receptor. Cell **46:**645–652.
14. **Hirschhorn, J. N., S. A. Brown, C. D. Clark, and F. Winston.** 1992. Evidence that SNF2/SWI2 and SNF5 activate transcription in yeast by altering chromatin structure. Genes Dev. **6:**2288–2298.
15. **Imbalzano, A. N., H. Kwon, M. R. Green, and R. E. Kingston.** 1994. Facilitated binding of TATA-binding protein to nucleosomal DNA. Nature (London) **370:**481–485.
16. **Johnston, R. F., S. C. Pickett, and D. L. Barker.** 1990. Autoradiography using storage phosphor technology. Electrophoresis **11:**355–360.
17. **Lee, D. Y., J. J. Hayes, D. Pruss, and A. P. Wolffe.** 1993. A positive role for histone acetylation in transcription factor access to nucleosomal DNA. Cell **72:**73–84.
18. **Li, B., C. C. Adams, and J. L. Workman.** 1994. Nucleosome binding by constitutive transcription factor Sp1. J. Biol. Chem. **269:**7756–7763.
19. **Li, Q., and Ö. Wrange.** 1993. Translational positioning of a nucleosomal glucocorticoid response element modulates glucocorticoid receptor affinity. Genes Dev. **7:**2471–2482.
20. **Lu, Q., L. L. Wallrath, H. Granok, and S. C. R. Elgin.** 1993. $(CT)_n$ $(GA)_n$ repeats and heat shock elements have distinct roles in chromatin structure and transcriptional activation of the *Drosophila hsp26* gene. Mol. Cell. Biol. **13:**2802–2814.
21. **Luisi, B. F., W. X. Xu, Z. Otwinowski, L. P. Freedman, K. R. Yamamoto, and P. B. Sigler.** 1991. Crystallographic analysis of the interaction of the glucocorticoid receptor with DNA. Nature (London) **352:**497–505.
22. **Maxam, A. M., and W. Gilbert.** 1977. A new method for sequencing DNA. Proc. Natl. Acad. Sci. USA **74:**560–564.
23. **McPherson, C. E., E.-Y. Shim, D. S. Friedman, and K. S. Zaret.** 1993. An active tissue-specific enhancer and bound transcription factors existing in a precisely positioned nucleosomal array. Cell **75:**387–398.
24. **Miesfeld, R., S. Rusconi, P. J. Godowski, B. A. Maler, S. Okret, A.-C. Wikström, J.-Å. Gustafsson, and K. R. Yamamoto.** 1986. Genetic complementation of a glucocorticoid receptor deficiency by expression of cloned receptor cDNA. Cell **46:**389–399.
25. **Muchardt, C., and M. Yaniv.** 1993. A human homologue of Saccharomyces cerevisiae SNF2/SWI2 and Drosophila brm genes potentiates transcriptional activation by the glucocorticoid receptor. EMBO J. **12:**4279–4290.
26. **Noll, M.** 1974. Internal structure of the chromatin subunit. Nucleic Acids Res. **1:**1573–1578.
27. **Perlmann, T., and Ö. Wrange.** 1988. Specific glucocorticoid receptor binding to DNA reconstituted in a nucleosome. EMBO J. **7:**3073–3079.
28. **Perlmann, T., and Ö. Wrange.** 1991. Inhibition of chromatin assembly in *Xenopus* oocytes correlates with derepression of the mouse mammary tumor virus promoter. Mol. Cell. Biol. **11:**5259–5265.
29. **Peterson, C. L., and I. Herskowitz.** 1992. Characterization of the yeast SWI1, SWI2 and SWI3 genes, which encode a global activator of transcription. Cell **68:**573–583.
30. **Pina, B., U. Bruggemeier, and M. Beato.** 1990. Nucleosome positioning modulates accessibility of regulatory proteins to the mouse mammary tumor virus promoter. Cell **60:**719–731.
31. **Pruss, D., F. D. Bushman, and A. P. Wolffe.** 1994. Human immunodeficiency virus integrase directs integration to sites of severe DNA distortion within the nucleosome core. Proc. Natl. Acad. Sci. USA **91:**5913–5917.
32. **Pryciak, P. M., and H. E. Varmus.** 1992. Nucleosomes, DNA-binding proteins, and DNA sequence modulate retroviral integration target site selection. Cell **69:**769–780.
33. **Reik, A., G. Schütz, and A. F. Stewart.** 1991. Glucocorticoids are required for establishment and maintenance of an alteration in chromatin structure: induction leads to a reversible disruption of nucleosomes over an enhancer. EMBO J. **10:**2569–2576.
34. **Richard-Foy, H., and G. L. Hager.** 1987. Sequence-specific positioning of nucleosomes over the steroid-inducible MMTV promoter. EMBO J. **6:**2321–2328.
35. **Richmond, T. J., J. T. Finch, B. Rushton, D. Rhodes, and A. Klug.** 1984. Structure of the nucleosome core particle at 7 Å resolution. Nature (London) **311:**532–537.
36. **Rusconi, S., and K. R. Yamamoto.** 1987. Functional dissection of the hormone and DNA binding activities of the glucocorticoid receptor. EMBO J. **6:**1309–1315.
37. **Scatchard, G.** 1949. The attractions of proteins for small molecules and ions. Proc. Natl. Acad. Sci. USA **51:**660–672.

38. **Scheidereit, C., and M. Beato.** 1984. Contacts between hormone receptor and DNA double helix within a glucocorticoid regulatory element of mouse mammary tumor virus. Proc. Natl. Acad. Sci. USA **81:**3029–3033.
39. **Schild, C., F.-X. Claret, W. Wahli, and A. P. Wolffe.** 1993. A nucleosome dependent static loop potentiates estrogen-regulated transcription from Xenopus vitellogenin B1 promoter in vitro. EMBO J. **12:**423–433.
40. **Shrader, T. E., and D. M. Crothers.** 1989. Artificial nucleosome positioning sequences. Proc. Natl. Acad. Sci. USA **86:**7418–7422.
41. **Simpson, R. T.** 1990. Nucleosome positioning can affect the function of a cis-acting DNA element in vivo. Nature (London) **343:**387–389.
42. **Simpson, R. T.** 1991. Nucleosome positioning: occurrence, mechanisms and functional consequences. Prog. Nucleic Acid Res. Mol. Biol. **40:**143–184.
43. **Straka, C., and W. Hörz.** 1991. A functional role for nucleosomes in the repression of a yeast promoter. EMBO J. **10:**361–368.
44. **Taylor, I. C. A., J. L. Workman, T. J. Schuetz, and R. E. Kingston.** 1991. Facilitated binding of GAL4 and heat shock factor to nucleosomal templates: differential function of DNA-binding domains. Genes Dev. **5:**1285–1298.
45. **Tsai, S. Y., J. Carlstedt-Duke, N. L. Weigel, K. Dahlman, J.-Å. Gustafsson, M.-J. Tsai, and B. W. O'Malley.** 1988. Molecular interactions of steroid hormone receptor with its enhancer element: evidence for receptor dimer formation. Cell **55:**361–369.
46. **Wrange, Ö., P. Eriksson, and T. Perlmann.** 1989. The purified activated glucocorticoid receptor is a homodimer. J. Biol. Chem. **264:**5253–5259.
47. **Yoshinaga, S. K., C. L. Peterson, I. Herskowitz, and K. R. Yamamoto.** 1992. Roles of SWI1, SWI2 and SWI3 proteins for transcriptional enhancement by steroid receptors. Science **258:**1598–1604.
48. **Zaret, K. S., and K. R. Yamamoto.** 1984. Reversible and persistent changes in chromatin structure accompany activation of a glucocorticoid-dependent enhancer element. Cell **38:**29–38.